



Finite Element Models for Predicting Moisture Effects on Bolt Embedment and Connection in Timber

Henry Meleki Kiwelu

Department of Structural and Construction Engineering, Collage of Engineering and Technology, University of Dar es Salaam, P.O. Box 35131 Dare es Salaam, Tanzania Email address: hekimaus2005@gmail.com

Received 12 March 2023 Revised 25 Aug 24, Accepted 25 Sept, Publ 31 Dec 2024

<https://dx.doi.org/10.4314/tjs.v50i5.1>

Abstract

The mechanical performances of timber connections are particularly important for timber engineers involved in the design of the wood structures. The mechanism of connection must be well understood in order to design a safer connection and avoid catastrophic failure. Often connections are made weak fuse elements by deliberate intent to ensure that if structural systems fail it will be by controllable ductile deformation of connections in load paths. Model method of determining engineering design capacities of laterally loaded dowel fasteners, such as bolts, screws and nails was developed. It should however be pointed out that FE and similar continuum model results always over predicted capacities at particular levels of deformation relative to experimental values. This result was expected and reflects the well-known inability of such models to incorporate all energy sinks that exist in experiments. The primary findings of the work reported is that it is highly viable to predict even complex effects that treatments like post-fabrication moisture conditioning have on responses of bolted glulam connections. Uniqueness of what is presented lies in the analysis of the combined influences of moisture content and mechanical loads by numerical methods. This makes such models viable means of supplementing physical test data and analyzing of highly complex timber connection situations.

Keywords: Timber Connections; Finite Element Models; Moisture Effects; Bolt Embedment; Mechanical Loads

Introduction

Finite element analysis has been widely applied to engineering problems, including analysis of connection for structural timber (Weckendorf et al. 2015). However, the number of publications relevant to effects of timber moisture history on physical and mechanical responses of structural elements and connections is limited. This paper focuses specifically on three-dimensional (3-D) Finite Element Models (FEM) of single bolt connection where in the bolt loads a glulam member parallel to grain (CSA 2014). The 3-D FE modelling of material property was also developed. That material property modelling was subsidiary to and precursory to

connection modelling and was the vehicle for gaining insights into how to model connections. The situations analyzed are highly complex due to factors like the anisotropic (assumed orthotropic) and hydroscopic nature of glulam (wood) as a material, geometric influences like oversized bolt holes and bending deformation of bolts that cause changes in the contact between bolts and glulam (Kiwelu 2019). It is for that reason that generalized FE techniques were adopted as a logical analysis method. Uniqueness of what was done relates mostly to inclusion of effects of moisture content variations in FE models. The specific scope of modelling covered by this study is the Connection test models for situations where

a single ½ inch (12.7 mm) or ¾ inch (19.1 mm) bolt loads a glulam member parallel to grain.

Differential movements most often calculated by engineers are those resulting from differentials in elastic compliances of interconnected parts in the structural system. Here emphasis is also on short term differential movements that occur due to differential dimensional responses of interconnected parts as the result of differentials in physical responses of materials from which parts are made (Khaurohf et al. 2005). The primary point of interest in the case of building superstructures manufactured by combining the timber products glued-laminated-timber (glulam) and steel are; aging, shrinkage and creep of glulam. According to Smith et al. (2015), Secondary interest is in hybrid building superstructures where glulam and steel are used in conjunction with reinforced concrete, RC elements. The physical processes are highly complex and the temporal variations in magnitudes of resulting strains and deformations in structural systems are strongly related to moisture movements within parts, ambient temperature and moisture exchanges between joined materials and between parts and surrounding air. It follows therefore that design and construction decisions and practices and environmental factors strongly influence differential movements within superstructure systems (Fournier et al. 2007).

Modelling

Constitutive Modelling

Wood is a complex fibre-reinforced composite which can be considered as orthotropic with three main directions namely longitudinal, radial and tangential directions. Each one of the orthotropic directions has mechanical properties that are different from the other and, in each direction the behaviour is also different in tension and in compression (Kiwelu 2017). Particularly in compression perpendicular to grain, timber shows ductile behaviour with appearance of the densification phenomenon. To describe accurately this

behaviour, there is a need to use anisotropic elasto-plastic law, based on the Hill's criterion and coupled with the ductile densification. The modelling approach is based on the thermodynamic approach of irreversible processes with internal variables developed in the context of large deformation theory for the three-dimensional continuum. According to literature, orthotropic material theory has been widely used as the best mathematical description of wood on a 3D macroscopic level. Orthotropic model includes the assumption that wood is a continuum, regardless of the differences between early wood and latewood, fibre porosity, and inherent discontinuities, such as knots, pith and ray. The orthotropic model only considers the difference of stress-strain relations according to the longitudinal, radial and tangential directions. The constitutive relationships in the three directions can be determined using the standard uni-axial loading tests. The linear elastic orthotropic model has been proven to work properly for Finite Element (FE) analysis for wood when wood behaves within an elastic range (Fournier et al. 2007).

Total strain vector ϵ_{total} can be divided into elastic ϵ_s , thermal induced strain, ϵ_T Moisture induced strain ϵ_U Creep strain ϵ_{CR} and mechanosoptive Strain ϵ_{MS}

$$\epsilon_{total} = \epsilon_s + \epsilon_T + \epsilon_u + \epsilon_{cr} + \epsilon_{ms} \quad (1)$$

The component ϵ_{CR} in eqn1 is a creep strain that would occur under constant climatic condition and component ϵ_{ms} is the incremental strain associated with climatic variations.

Elasticity Based Model

In the 3D FE modeling of wood material, the available model reported was the linear elastic transversely isotropic model in which the assumption of plane symmetry was added to the orthotropic model. For wood behaviour within the proportional limit, this model produces acceptable results. Smith et al. 2015 used the transversely isotropic model for wood to study the performance of various mortise and tendon joints using a 3D

FE model. Since the main objective of his study was to optimize the geometry of the mortise and tendon joints through a 3D FE parametric study, simulated results within the linear elastic range of the connections were sufficient. However, no consideration of the crushing behaviour for wood-to-wood contact resulted in the prediction of stiffer results than were observed in the experimental results.

(Jockwer 2014) developed a 3D FE model for a hollow dowel connection in glued-laminated timber that was locally reinforced by densified veneer wood (DVW). In this connection, the deformation of the timber member could be assumed to remain within the elastic range, because the timber member was sandwiched between the DVW reinforcements and a tube-type dowel connector was used to induce the failure at the connector itself in a ductile manner. This study showed that, if a given connection did not involve too much local nonlinear compression failure, use of the linear orthotropic elastic model for wood may be suitable for a 3D FE connection model.

For a general dowel-type connection however, the nonlinear behaviour of the wood should be taken into account for predicting the full load-deformation response. For these cases, (Smith et al. 2015) proposed a 3D FE nonlinear material model for wood. Based on the elastic orthotropic model, tri-linear constitutive relationships were fitted to parallel to grain compressive stress-strain curves and shear stress-strain curves which were incorporated into the transversely isotropic elastic material model for modeling bolted connections. The major shortcoming of this tri-linear model was that it needed a process for finding the fictitious material parameters, including Poisson's ratio and breakpoints in the tri-linear curves. If the parameters were not defined properly, negative stiffness coefficients could occur on the diagonal terms of the stiffness matrix, creating a problem in the convergence to the solution. However, it is an interesting model, because it was mentioned as the first 3D finite solid element nonlinear material model for wood

connections.

In order to trace the nonlinear stress-strain relationship more accurately, function-based methods were devised, rather than piecewise linearization methods. According to Smith et al. (2015) investigated a two-dimensional incremental-iterative secant stiffness approach and (ANSI. 2012 and APA 2010) expanded this approach to a 3D nonlinear orthotropic finite element material model for wood. Using power functions of a ratio between incremental-iterative stresses, they developed a model to update the change in modulus of elasticity in order to track the nonlinearity of the stress-strain curve. The model showed good simulations of the uniaxial load-deformation curves in shear and compression because the nonlinear parameters of the power function were determined from the experimental shear and compression data for the given species. However, with this model no attempts were made to predict the behaviour of a wood connection, which usually includes a very complex stress state (Kiwelu 2017).

Basically, the elasticity-based model is limited in that it can only predict reversible strains. The results of the elasticity-based models can only be justified within the elastic response of the wood. However, in reality the nonlinear response of wood comes mainly from the permanent deformation of wood fibres, which is a non-conservative and path-dependent phenomenon. Therefore, to overcome the limitation of the elastic model, the development of a plasticity theory-based model should be considered.

Numerical Modelling for Bolt

Finite element (FE) methods are nowadays widespread and much-used tools to model the mechanical behavior of a structure on which a set of known external variables, forces or prescribed displacements, are acting. A set of partial differential equations are solved numerically to determine the values of the unknown internal variables, namely the displacements. From displacements, the strains can be calculated, and for example in the linear elastic domain using Hooke's law, also the stresses. This

last step, from strains to stresses is done by applying a valid constitutive law. The modelled structure is split into a system of smaller, finite elements for which the system of equations is approximately solved. Applying boundary conditions such as displacements of some of the nodes, the single smaller elements are connected with each other and a solution for the whole system can be approximately determined (ANSI 2012).

Due to the importance of the problem, bolted joints have previously been studied by using numerical modelling. Weckendorf, et al. (2015) developed a nonlinear numerical model to study the behaviour of timber connections with relatively low member thickness-to-fastener diameter ratios. A plasticity-based compressive constitutive material model was proposed to represent wood as an elasto-plastic orthotropic material in regions of biaxial compression. Linear elastic orthotropic material response was used with maximum stresses taken as the basis for predicting failure criteria. Nonlinear geometry due to increased sliding contact between the bolt and the hole was modelled using the Lagrange multiplier algorithm (Zhang et al

2023)

General Aspects of FE Modelling

Contemporary modelling tools like ABAQUS have been widely verified as being robustly reliable for modelling complex structural engineering problems. Yet, it still remains a skilled specialist task to utilize such tools because such programme (s) have to be correctly directed to set up and solve the partial differential equations that represent specific physical situations, e.g. deformation responses of mechanical connection to external loading. Therefore, although different analysts may use the same analytical software to model the same situation, the quality of the predictions they produce will vary. In large part this reflects that FE models provide approximate solutions over entire physical domains that are modelled and solutions are sensitive to meshing strategies employed, and to time marching strategies in the case of analyses in which there is a time argument within the formulation of a model (Kiwelu 2019). Figure 1. defines the general nature of any FE analysis. In figure 1 below represent the process involved in modelling any Finite element analysis step by step.

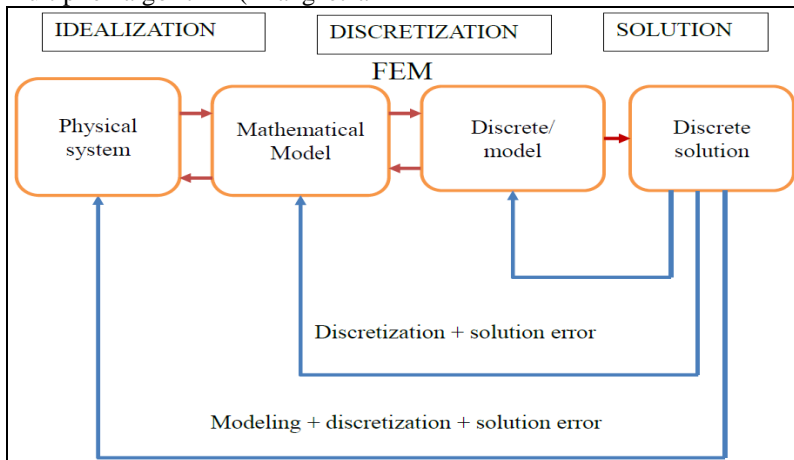


Figure1: Finite Element Modelling process

Material Numerical Models

Version 6.12 of ABAQUS (APA,2010) was used to create FE models representing

the behavior of wood loaded in different directions of material symmetry, including embedment strengths of bolts. In models constraints from a master node were

distributed to other nodes required to have the same displacement or load so that ABAQUS would produce ‘perfect’ load versus deformation curves.

Except when explicitly mentioned otherwise FE stress analyses were performed based on assuming the mechanical properties listed in Table 1 with those properties setting the presumed scaling ratios between elastic constants.

Bolt embedment specimen models mimicked the half-hole test arrangement. The glulam specimen was modelled as having an unloaded thickness of $1.5d$, where d is the bolt diameter. Conceptually the representation follows the wood foundation modelling strategy Model presented by Magistris et al. (2008) resulting in definition

Table 1: Material properties

Notation	Property	Value	Unit
E_r	Elastic modulus	370	MPa
E_t		370	MPa
E_l		10300	MPa
V_{rt}	Poisson Ratios	0.558	-
V_{rl}		0.038	-
V_{tl}		0.12	-
G_{rl}	Shear Modulus	640	MPa
G_{lr}		640	MPa
G_{rt}		64	MPa
δ	Initial Density	490	Kg/m ³
T	Initial temperature	21	°C
u	Moisture content	8,12,17	%
α_{ur}	Coefficient of moisture expansion	0.13	-
α_{ul}		0.27	-
α_{ut}		0.005	-
E_s	Youngs modulus of steel	200000	MPa
V_s	Poisson modulus for steel	0.33	-

Subscript notation:

x, y, z = model space coordinate directions

r, t, l = radial, tangential and longitudinal directions in glulam, coincident with x, y, z respectively.

Material Modelling Results

Figures to 2 show examples of predicted behaviors of embedment specimens where bolts load glulam either parallel or perpendicular to grain, with figure 2, 3, 4 and 5 including comparisons of FE model and average experimental load versus embedment responses. As can be seen,

of a Radius of Wood Foundation R equal to $1.8d$. Orthotropic material properties used to model the foundation zone are defined in Table 1 model the foundation zone is defined in Several mesh size strategies were investigated, to ensure that final outputs were convergent with exact results. The final mesh employed had 18,630 nodes and 16,285 elements. Contact between the bolt and glulam was modelled using contact pair surface with glulam treated as slave surface and bolt surface treated as master surface since it is stiffer than wood. Boundary condition were that the bottom surface of the glulam specimen was fixed and load applied to the top of the half-bolt.

agreement between shapes of FE model and experimental response curves is excellent. However, the model results always overestimate the load corresponding to an embedment deformation, including strength, with the overestimate being in the order of 10 to 15%.

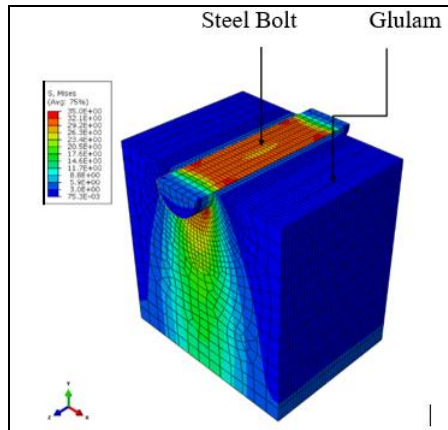


Figure 2: von Mises stresses in glulam embedment specimen loaded perpendicular to grain by 1/2 inch bolt, moisture content at 12 percent test percent

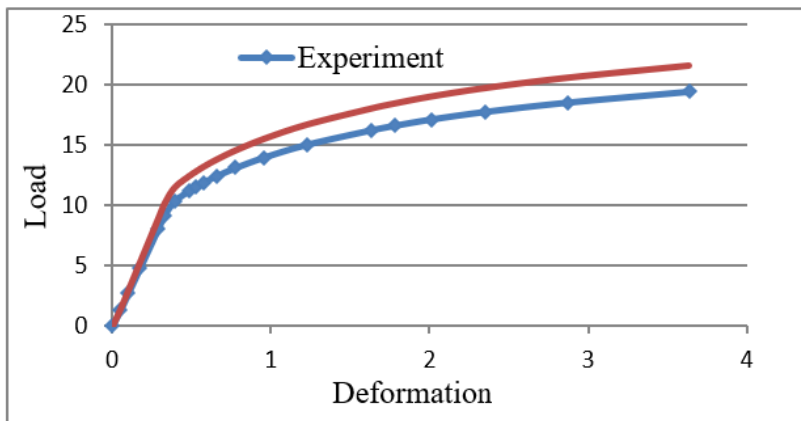


Figure 3: Load – embedment response for glulam loaded parallel to grain by 1/2 inch bolt, moisture content at test 12 percent

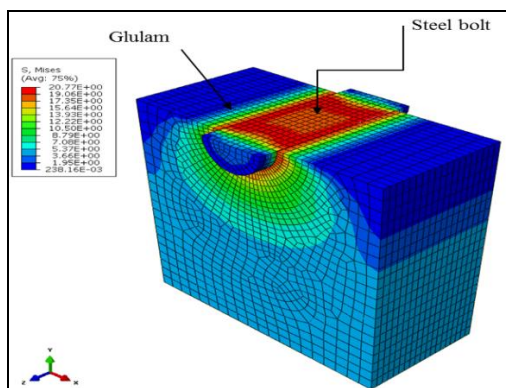


Figure 4: von Mises stresses in glulam embedment specimen loaded perpendicular to grain by 3/4 at 12 percent moisture content

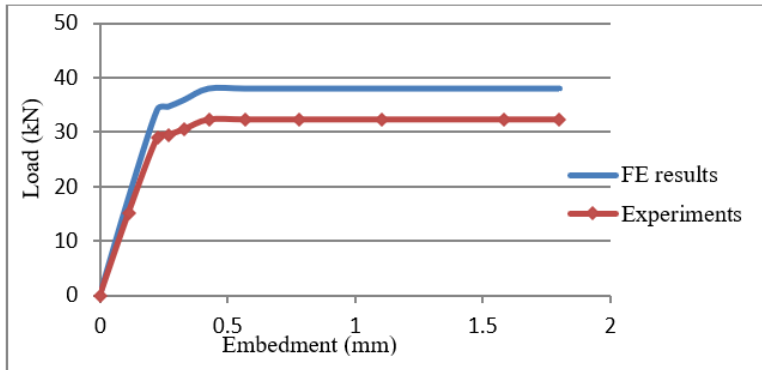


Figure 5: Load embedment response for glulam loaded parallel to grain by 3/4 inch bolt, moisture content at test 12 percent

The results from all FE embedment analyses are discussed there in the context of using the approach to supplement or plan experimental investigations. However, from the perspective of this study research the main value was that the approach employed was shown to be viable for modelling glulam elements in bolted connections, i.e. cases where modelling must handle additional complexities.

Tension Parallel to Grain Loading

During development of the parallel to grain tension the mesh was refined several times until there was no change in the results, with the meshing strategy focused on proper modelling of stress concentration caused by the necked geometry of specimens. In total there were 23,264

elements and 36,444 nodes, Figure 6. The applied boundary conditions were prevention of movement of surface nodes at the bottom end of the specimen at locations corresponding to where the lower jaws of the test machine gripped physical specimens. Load was applied as equal vertical displacement of surface nodes at the top of the specimen corresponding to where the upper jaw of the test machine gripped physical test specimens. Figure 7 shows the predicted load – elongation relationship and compares it with the average experimental response. The definition of extension used is 1.2mm. As seen the model overestimated stiffness and strength be about 10 percent.

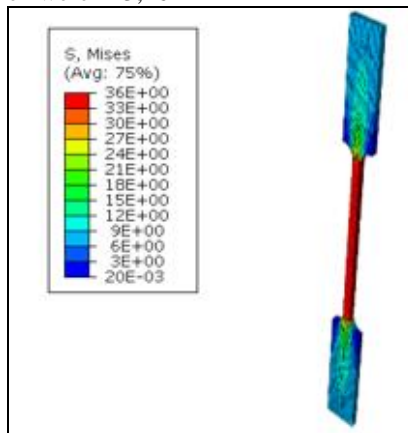


Figure 6: von Mises stresses in parallel to grain glulam tension test, moisture content at test 12 percent

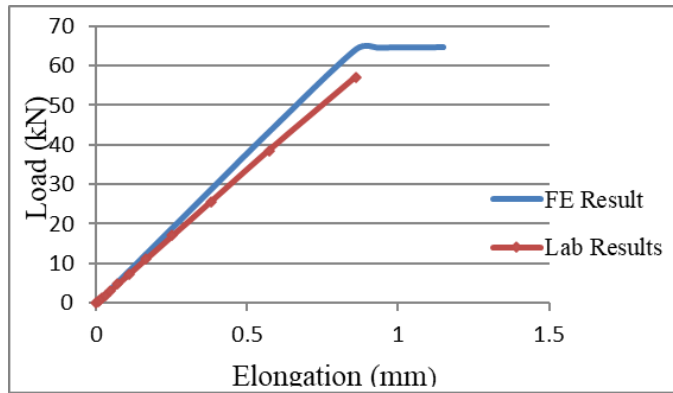


Figure 7: Load - elongation response for tension parallel to grain glulam specimen, moisture content at test 12 percent *Perpendicular to Grain Loading*

The approach takes to model tension perpendicular to the grain specimens was similar to that for tension parallel to grain specimens, with the exception of how the ends of the specimen were constrained or loaded. Applied boundary conditions were to assume that the bottom of the specimen is fixed at the lower surface and to apply a uniform surface pressure (sectional) to the upper surface. As shown in Figure 8 boundary conditions are not truly reflective of the physical way in which specimens were loaded. This is believed justified because specimens always fail at or close to the specimen neck and therefore the requirement is to mimic the stress at that location in a satisfactory manner, which can

be done in the described way because away from the neck and where load is applied the specimen is locally very rigid. The model used had 62,200 elements and 270,873 nodes. The definition of extension used is 1.2mm. As for tension parallel to grain the model overestimated stiffness and strength, with in this case the errors being about 10 and 25 percent respectively. In this new instance the attributed reason for stiffness overestimation is the same, but the more considerable overestimation of strength is attributed to well-known difficulties associated with manufacture of representative perpendicular to grain test specimens, and the need to use fracture mechanics rather than continuum mechanics analysis to accurately model the situation.

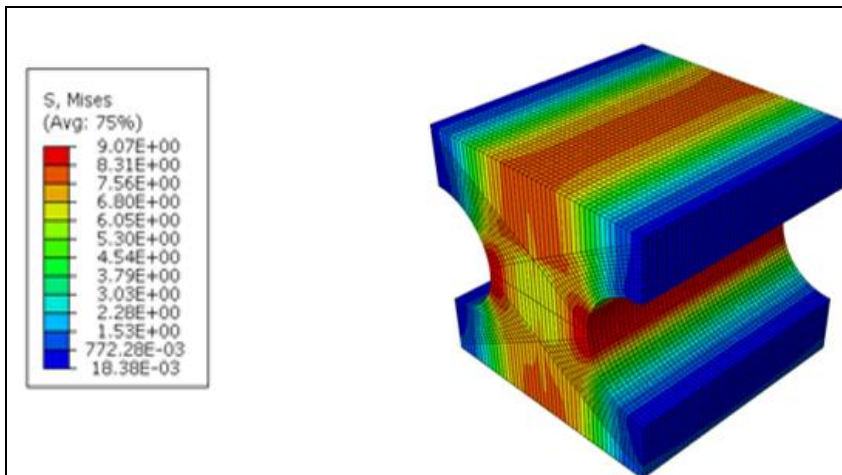


Figure 8: von Mises stresses in perpendicular to grain glulam tension test, moisture content at test 12 percent

Compression Response Parallel to Grain Loading

A compression specimen model was developed to replicate what is always done at the laboratory experiments as closely as possible. The thick steel two plates were modelled in contact with glulam specimen to represent load and reaction platens in the test arrangement, with those plate rather than the specimen ends subjected to uniform pressure representing the effects of the load applied by the test machine. As with embedment models Type C3D20R-a 20-node reduced integration quadrilateral isoperimetric brick elements with three degrees of freedom at each node were used, in this case to create the prismatic glulam specimen and steel bearing platens in a modelling space, Figure 9. The number of elements used was to

represent the glulam was 46,875 with 20,0876 nodes. As in actual tests displacement-controlled loading was used by applying vertical displacement at the top surface. Contact surfaces between the steel blocks and glulam specimen were modelled with general contact and assuming a coefficient of friction of $\mu= 0.7$ (Smith et al, 2003) . Mesh convergence was identified for all the compression models by checking the convergence of the simulated load-deformation curves by assuring there was no change of the result by refining the model. The nodes on the bottom surface of the model (i.e. bottom steel plate) were fixed as a boundary condition. Displacements were then applied at the top plate. Predicted von Mises stresses and the load-displacement curve are as presented in Figures 9.

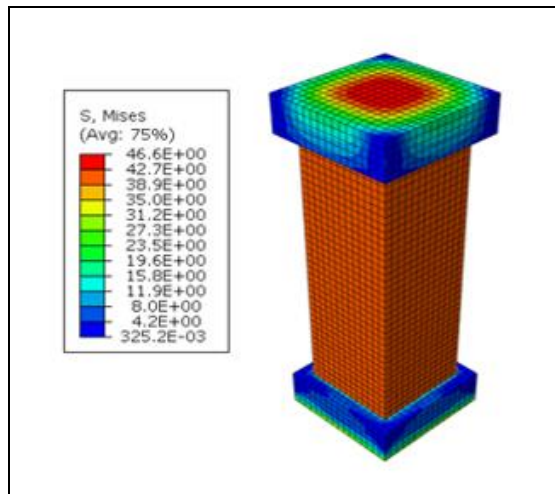


Figure 9: von Mises stresses for glulam loaded in compression parallel to grain, moisture content at test 12 percent

Perpendicular to compression Grain Loading

The perpendicular to grain model was developed along the same lines as the parallel to grain model, but taking account of the full-face support at the bottom surface and the partial face loading at the top surface, to mimic the physical test arrangement, Figure 10. This model had

46,875 elements and 51,376 nodes, which was found sufficient to produce convergent solutions, resulted in the load-displacement response in Figure 11. The results graph also shows the associated experimental average load-displacement relationship. As seen the model over predicted stiffness and strength by about 10 %.

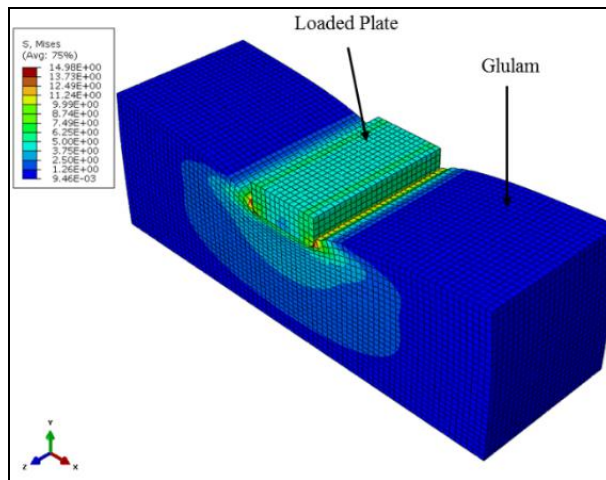


Figure 10: Model and stress Parten for glulam loaded in compression perpendicular to grain, moisture content at test 12 percent.

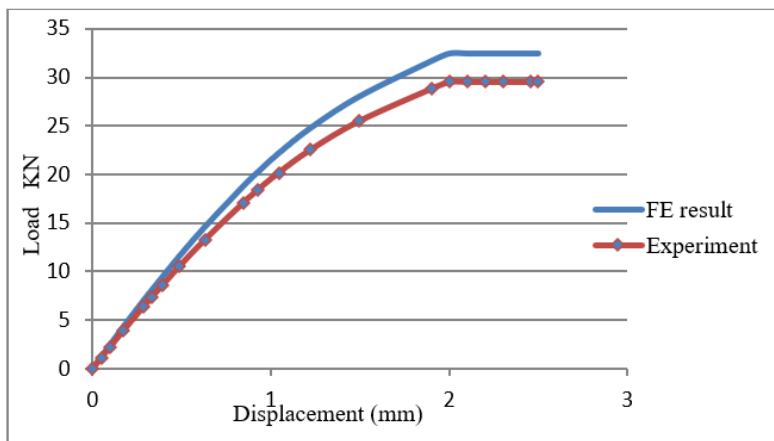


Figure11: Load - displacement response for glulam loaded in compression perpendicular to grain, moisture content at test 12 percent

Shear Response

The shear response model largely mirrored the compression parallel to grain model, with the exception that it was required to account for the more complexity and to incorporate lateral restraints to prevent rotational instability due to the asymmetric geometry in the zy plane, Figure 7 the model

had 19,400 elements and 21,710 nodes, which were to obtain convergent solutions. The predicted load – displacement response is shown in Figure 12 with the displacement corresponding to 1.1mm. As in other situations, the model overestimated strength, and by about 15 percent.

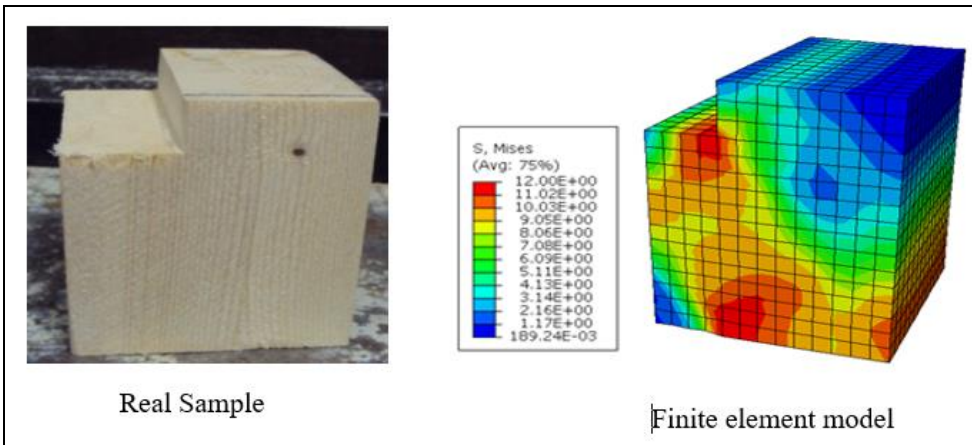


Figure 12: von Mises stresses in perpendicular to grain glulam tension test, moisture content at test 12 percent

Summary of Derived Material Properties

The thematic findings running through the reported FE analyses were:

- Models mimic shapes of load deformation relationships very well in terms of the non-linearity prior to peak load. This implies that the use of 3D continuum analysis in conjunction with the von Mises yield equation is acceptable for representing the behaviour of glulam up to peak load.
- Models overestimate stiffness and strength of test specimens. The discrepancy lies in the order of 10 to 15 percent for all investigated situations, with the exception of tension strength perpendicular to grain (for which the discrepancy is greater).

Above it is maintained that overestimation of stiffness and strength is at least partly attributable to irregularities associated with lack of material or geometric symmetry, with material asymmetry always existing in glulam/wood test specimens. This reflects that material like glulam contains many structured and semi-random intra-component asymmetries at wood feature levels (Smith et al. 215). In support of the contention is extensive work done at the University of Maine, USA with researchers there having used discrete element modelling techniques (that are cumbersome in general but well suited to the particular purpose) to demonstrate conclusively that

the explanation advanced here is technically correct (Fournier et al. 2007)

Table 4.3 shows selected maximum/peak capacities of specimens determined based on laboratory tests and FE analysis and averages ratios of those values, with those comparisons applying to situations where moisture contents at test were 12 percent. The ratios (of test values indexed to FE values) are the factors by which model predictions would have to be multiplied before being used to predict average engineering strength properties.

Overview of Models

This section of the thesis presents 3D nonlinear finite element modelling developed to simulate structural behavior of glulam connections subjected to static loading at different moisture conditions, including failure. The modelling presented is specific to cases where bolts nominally bear on glulam parallel to grain because that is an orientation of primary interest for structural design. Also, consideration is restricted to single bolt connections. In principle the same approach can be applied to cases where bolts bear on glulam (or other wood products) at other directions relative to grain, and to connections with multiple bolts. Originality of what is included here is mainly in respect of application of FE modelling to situations where connections are moisture conditioned after fabrication but prior to application of external load.

As already noted, early FE modelling of bolted timber connections was based on 2-D analysis which in practice meant applicability was to connections that are geometrically symmetric and concentrically loaded, and that have wood members thin enough that bolt bending deformation is negligible. Often realistic bolt connections create situations where there is substantive bolt bending deformation and therefore 3-D analyses are required for accurate results. Thus, in this study a 3-D FE model was developed using the ABAQUS software package. Because connections modelled were geometrically symmetric, only one quarter of the actual geometry was actually modelled in the FE model spaces. External boundary conditions applied to the connection meshes were

associated with symmetry and those associated with mechanical and moisture loads.

Mechanical loading was applied by imposing equal monotonically increasing extension displacements at one end (nominally the top surfaces) of the connection meshes and anchoring the meshes at the other end (nominally the bottom surfaces). As shown in Figures 13 and 14 the boundary conditions applied corresponded to all nodes in a top surface of steel plate member being displaced in the x direction and zero displacement of all nodes on the bottom of the glulam members in the x direction. Displacement was applied incrementally in order to obtain well-defined load-slip curves.

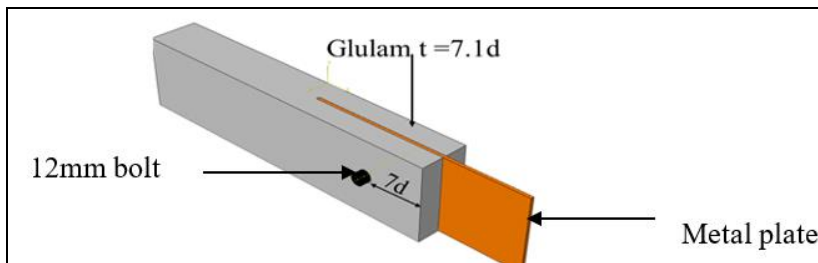


Figure 13: Assembled full model of a connection with a $\frac{1}{2}$ inch bolt

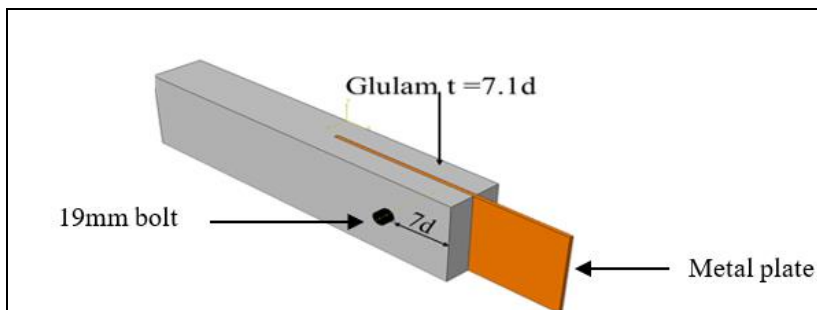


Figure 14: Assembled full model of a connection with a $\frac{3}{4}$ inch bolt

The modelling of the material property nonlinearity and bolt-to-glulam contact analysis necessitated high refinement of FE meshes model, resulting in large computer storage and running time requirements. The connection domain was broken down into three primary components: the bolt, the glulam member and the steel plate member.

Initially those three components were modelled separately and then they were assembled into a full system representation, with the assembly stage involving addition of interfaces between parts. Contact surfaces created at interfaces included ability to handle contact between the bolt and glulam member, between the bolt and the steel

plate, and between the glulam member and the steel plate.

Models matched the exact conditions in the laboratory, and were run at the three moisture contents at test of 8, 12 and 17 percent. Assumptions made were:

- because glulines were observed to remain intact during tests.
- Glulam is homogeneous and free from gross features like knots and resin pockets. This is acceptable because in tests bolts were only located within clear wood areas of glulam.
- Bolts and steel plate members respond as isotropic perfect elasto-plastic materials. This is acceptable because in tests non-linearity was observed to be associated with glulam deformation.

Load application

Load can be introduced to a model by deformation (or displacement) control where, for instance, a point(s) in one component in a model is moved a prescribed deformation over a certain time step relative to a point(s) in another component. Such relative movement between bodies results in a force flow between them. Use of deformation control load application is very useful when the response of a system is nonlinear. A load can be applied instantaneously i.e. in the beginning of an analysis step, or applied stepwise to simulate

- Glulines within glulam have negligible influence on that materials characteristics and therefore they do not need to be modelled. This is acceptable

ramped load application.

Single bolt model results

Selected results are shown below for von Mises stresses and deformed shapes as predicted by FE models of connections with a 1/2 inch bolt (Figures 15 to 17) and connections with a 3/4 inch bolt (Figures 18 to 20). Those figures represent nominal moisture contents at the time of loading of 8, 12 and 17 percent. The diagrams in each figure show quarter connection models defined by planes of symmetry of the full geometry. Mechanical load levels associated with the figures are for 6mm. The deformations and von stresses shown are for the steel plate member being pulled to the right relative to the glulam member, i.e. connections loaded in tension. For the connection with nominal moisture contents of 8,12 and 17 percent those results are coupled influences applied displacements and post-fabrication moisture conditioning of glulam members.

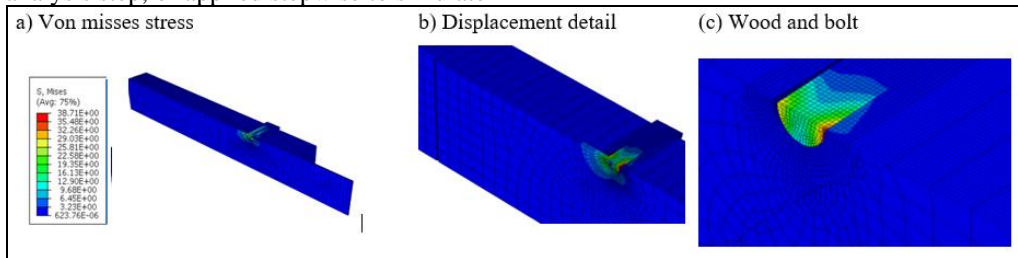


Figure 15: Connection with 1/2 inch (12.7 mm) bolt loading glulam parallel to grain, moisture content at test 8 percent

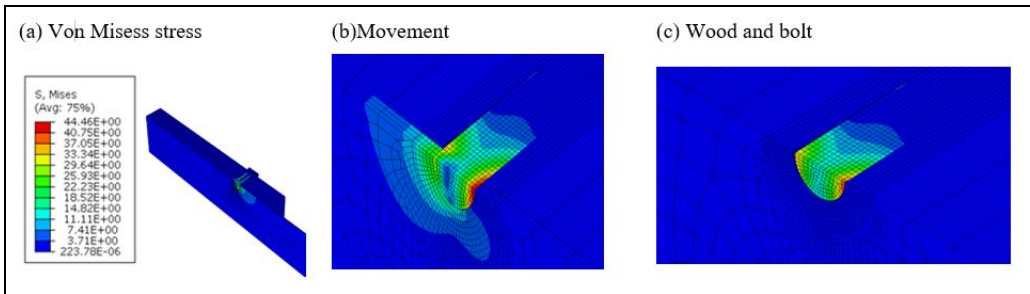


Figure 16: Connection with 1/2 inch (12.7 mm) bolt loading glulam parallel to grain, moisture content at test 12 percent

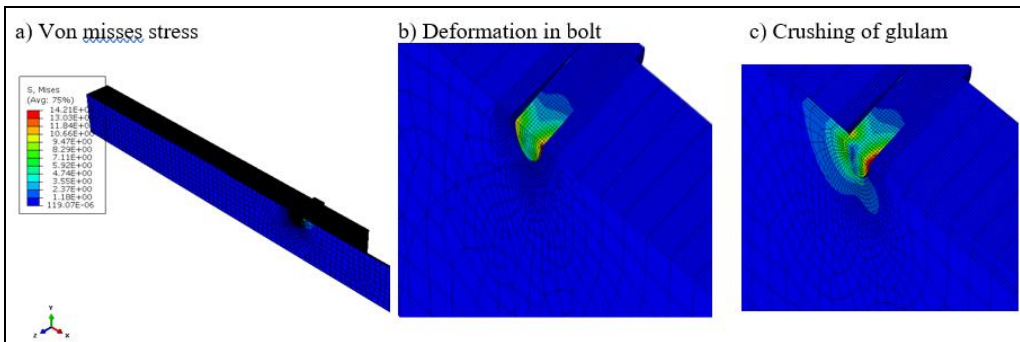


Figure 17: Connection with 1/2 inch (12.7 mm) bolt loading glulam parallel to grain, moisture content at test 17 percent

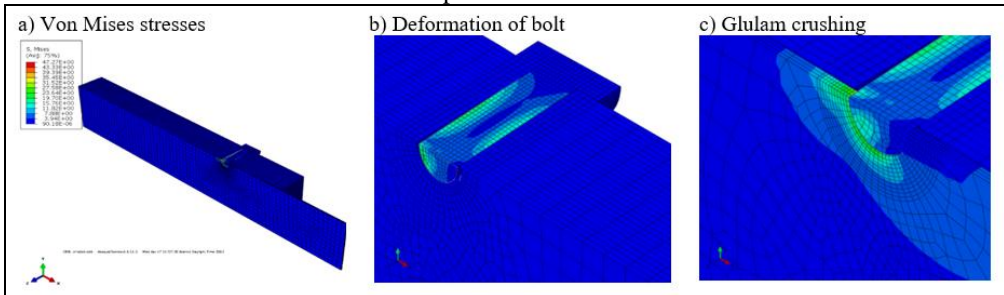


Figure 18: Connection with 3/4 inch (19.1 mm) bolt loading glulam parallel to grain, moisture content at test 8 percent

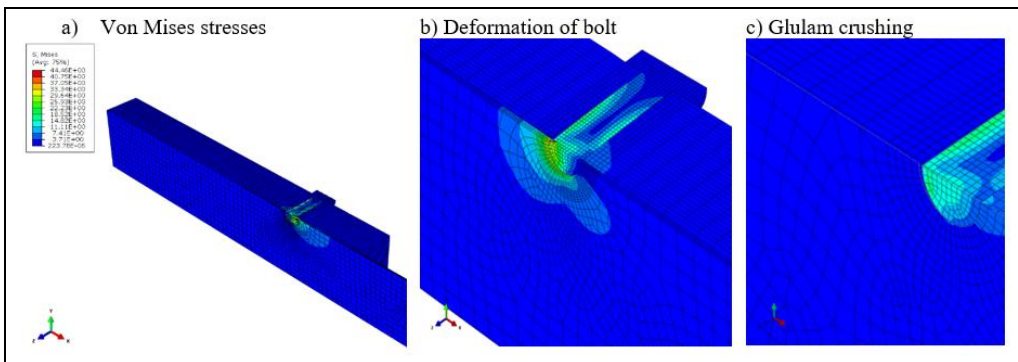


Figure 19: Connection with ¾ inch (19.1 mm) bolt loading glulam parallel to grain, moisture content at test 12 percent

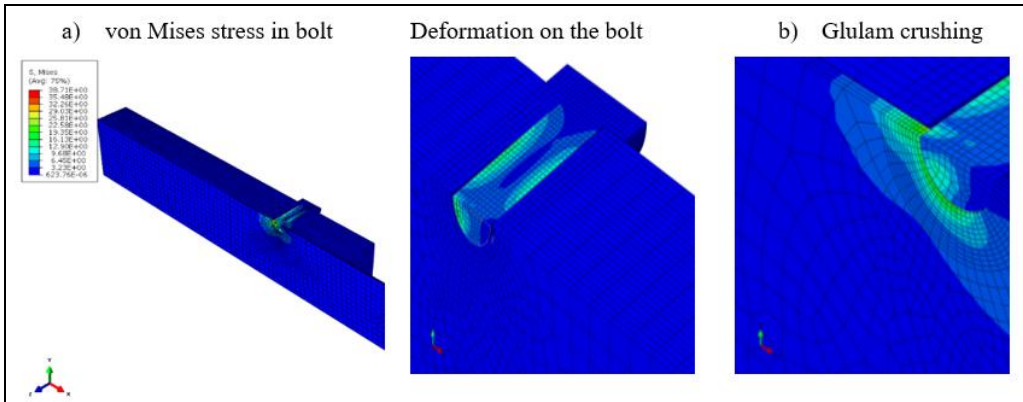


Figure 20: Connection with 3/4-inch (19 mm) bolt loading glulam parallel to grain, moisture content at test 17 percent

Comparison between laboratory and numerical modelling

Here results of three-dimensional (3D) finite element models of single bolt connections as presented are compared to matched experimental results presented. The objective of this is to illustrate the general level of accuracy achieved and to validate the suitability of FE models to predict coupled influences that moisture conditioning and mechanical load have on deformation and load carrying capacities of such connections. If successful this becomes an important step toward generalised mechanosorptive analysis of

complex timber engineering problems, and establishment of reliable numerical techniques that supplement what can be achieved via experimentation alone.

Load-displacement Response Comparison

Average experimental (EXP) load-displacement responses and corresponding finite element (FE) responses for connections with ½ inch (12.7mm) and ¾ inch (19.1mm) bolts are compared in Figures 3.1 and 3.2 respectively. In those comparisons displacement is taken to be 6mm that was taken to be an average observation from laboratory experiments.

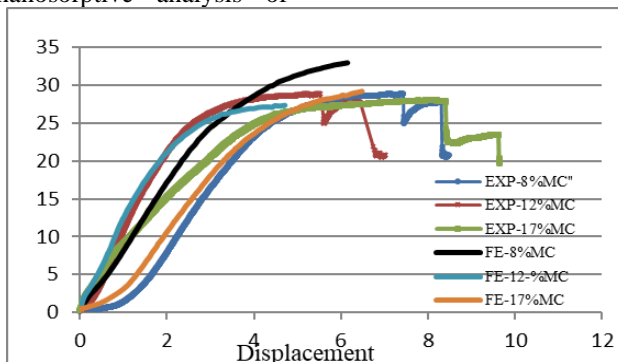


Figure 21: Comparison between FE and experiment load-displacement responses for connections with a ½ inch (12.7 mm) bolt

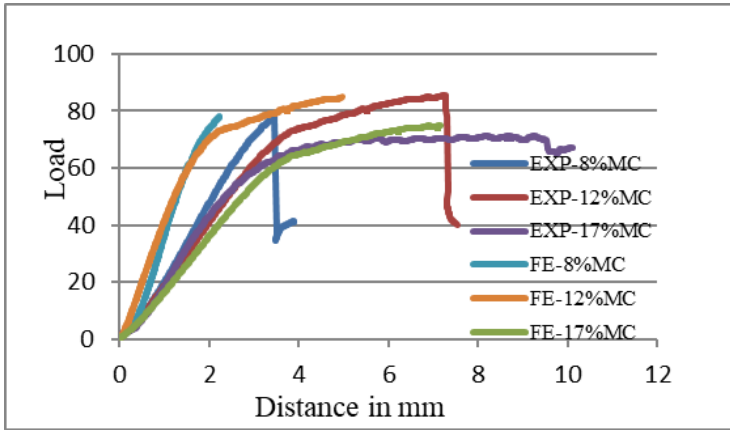


Figure 22: Comparison between FE and experiment load-displacement responses for connections with a 3/4 inch (19.1 mm) bolt

In respect of development of such contact the FE models start with the bolt in contact with sides of bolt holes that they will initially at least (i.e. prior to and bending deformation of bolts) load compressively. In experiments there are additional sources of initial nonlinearity associated with irregularity of shapes and alignments of bolt holes, and a random initial location of bolts within the tolerance holes into which they are inserted. It follows that in a quantitative sense comparison of raw EXP and FE in

particular load-displacement responses is not highly meaningful.

The quantitative comparisons chosen here to properly assess practical applicability and validity of the FE bolted connection models is to compare average experimental initial tangent stiffness (K) and 5 percent fastener diameter offset proportional limit loads (P_{pl}) determined from EXP and FE data using the methods. That comparison is shown in Table 2.

Table 2: Comparison of Mechanical properties of single bolt connections based on EXP and FE data

Specimen type	Bolts		Glulam		K (kN/mm)		P_{pl} (kN)	
	d (mm)	#	t (mm)	u (%)	EXP	FE	EXP	FE
B12-S-8	12.7	1	90	8	13.5	14 (1.0)*	26.9	27(1.0)*
B12-S-12	12.7	1	90	12	12.3	12.8(0.96)	25.2	27(1.1)
B12-S-17	12.7	1	90	17	10	10 (1.0)	21.9	27 (1.2)
B19-S-8	19.1	1	130	8	30	65 (2.2)	73.5	80(1.1)
B19-S-12	19.1	1	130	12	25	60 (2.4)	69.8	75(1.07)
B19-S-17	19.1	1	130	17	27	22 (0.8)	67.0	70 (1.05)

* Ratio of EXP value.

Based on Table 2 it can be concluded:

- FE models tend to overestimate stiffness and strength because models do not incorporate all energy sinks present in real connection experiments. This mirrors the findings and conclusions reported in for material test models.
- The FE model for connections with a 1/2 inch (12.7mm) bolt estimates initial

- displacement very well including when the glulam member is wetted or dried between times of fabrication and loading.
- The FE model for connections with a 3/4 inch (19.1mm) bolt does not estimate initial displacements very well irrespective of whether the glulam member is or is not moisture conditioned between the times of fabrication and

- loading. The discrepancies are inconsistent.
- FE models predict the proportional limit load for connections with a 1/2 inch (12.7mm) or 3/4 inch (19.1mm) bolt well (mostly to within 10 percent), including when the glulam member is wetted or dried between times of fabrication and loading.
 - In general shapes of FE model load-displacement curves match those of experimental curves. However there was difficulty with obtaining convergent numerical solutions beyond the point where materials in the stiffest models ($d = 19.1$ mm, $u = 8$ percent) because in that situation the ABAQUS equation solver subroutine struggled to solve the relatively poorly conditioned system equations. This leads to the conclusion that it is only reliably feasible to use models (of the type discussed) to predict engineering response parameters such as ductility ratios when bolts/fasteners are quite slender, because it is only for such cases that system equations within FE model remain well conditioned throughout analyses.

The discrepancy between FE model abilities to predict initial displacements well for connections with different size bolts is attributed to relatively proportion of overall displacement that is attributable to bolt bending deformation and the relatively small absolute magnitudes of displacements prior

Table 3: Comparison of embedment strength parallel to laminates at different moisture contents (MPa)

Specimen	Embedment tests	FE model	Canadian code	Eurocode 5
E-12-8-	35.9	35.0	25.1	44.1
E-12-12-	32.9	30.2	25.1	44.1
E-12-17-	28.8	29.2	16.8	36.36
E-19-8-	38.1	37.3	23.3	40.85
E19-12-	34.9	35.3	23.3	40.85
E-19-17-	24.7	26.4	15.6	33.42

The conclusions derived from the comparisons are:

- FE modelling determines embedment strength properties very accurately,

to wood crushing (beneath bolts) that occur for connections with a 3/4 inch (19.1mm) bolt.

Embedment Strength and Design Capacity Predictions

The glulam property used by design codes as the basis of predicting capacities of single bolt connections is embedment strength. Table 3 below compares glulam embedment strengths obtained directly from experiments FE model predictions, and values from the Canadian and Eurocode 5 timber design codes (CSA, 2014 and Kiwelu 2019). The basis of comparison is to assume a uniform stress distribution across the projected width of a bolt at the peak stress location in the length. The Canadian code values approximate to 5 percentile exclusion values, while the test, FE analysis and Eurocode 5 values approximate to 50 percentile exclusion values higher than Canadian code for timber engineering. Assuming that coefficients of variation for embedment strengths are in the order of 10 to 15 percent (Table 3), test, FE and Eurocode values should be about 1.2 to 1.3 times Canadian code values. [Note: The glulam density used to estimate Eurocode 5 embedment strengths was an average values and so corresponds approximately to 50 percentile exclusion embedment strengths.

including effects of any moisture conditioning of glulam.

- Allowing for differences associated with 5 versus 50 exclusion level bases of

values, the Eurocode 5 embedment strengths for the reference case of connections fabricated dry and tested at the same moisture content (specimens E-12-12-|| and E-19-12-||) code values tend to be slightly conservative.

- Generally the Eurocode 5 estimates are higher compared with test values. Possible reasons might include the slackness of the bolt in the hole in laboratory test and use of the half-hole test method.

Conclusions

The author successfully predicts bolt embedment strength and deformations of laterally loaded bolted connections in glued-laminated-timber (glulam). The unique aspect of the work was the coupled treatment of influences of glulam moisture content variations between when connections are fabricated and when they experience application of potentially damaging effects of external mechanical loads. Such situations are common for glulam superstructures of buildings in Tanzania and elsewhere. Primary specific conclusions are: Material models of glulam based on continuum mechanics representations can predict mechanical deformation and strength observed during modelling. This gives confidence to apply the von Mises material model to predict the behaviors of bolt embedment and bolted connection specimens. The short-term bolt embedment response of glulam can be predicted to good accuracy using continuum mechanics methods, provided that close attention is paid to proper modelling of the nonlinearity of the glulam material responses, the geometrically nonlinear development of the bolt-to-glulam contact surface, and the slip-stick nature of the bolt-to-glulam contact surface. Changes in displacement and strength responses of bolted connections in glulam that result from combined influences of moisture conditioning that occurs between times of fabrication and loading, and effects of mechanical external loads can be predicted to good accuracy using continuum

mechanics methods.

References

- ANSI. 2012 National design specification for wood construction. ANSI/AWC NDS-2012, ANSI, Washington, D.C.
- APA – The Engineered Wood Association (APA) 2010 Field notching and drilling of glued laminated timber beams. *Technical Note EWS S560G*, APA, Tacoma, Washington.
- Canadian Wood Council (CWC) 2010 *Wood design manual*. CWC, Ottawa, Ontario.
- CSA 2014 Engineering design in wood. CSA Standard 086-14, CSA, Ottawa, Ontario.
- Fournier, C.R, Davids, W.G., Nagy, E. and Landis, E.N 2007M morphological Lattice Models for the Simulation of Softwood Fracture and Failure, *Holzforschung, Walter de Gruyter*, 61: 360-366.)
- Jockwer, R. 2014 Structural behaviour of glued laminated timber beams with unreinforced and reinforced notches, Doctor of Science Thesis, *Eidgenössische Technische Hochschule Zürich*, Zurich, Switzerland.
- Kharouf Nourhene , McClure Ghyslaine ,and Smith Ian,2005 Post-elastic behaviour of single- and double-bolt timber Connections M.ASCE\2005 *J. Struct. Eng.* 131(1): [https://doi.org/10.1061/\(ASCE\)0733-9445\(2005\)131:1\(188\)](https://doi.org/10.1061/(ASCE)0733-9445(2005)131:1(188))
- Kiwelu, H. M. 2017. Moisture induced deformations in glulam members - Experiments and 3-D Finite Element Model. *Tanzania J. Eng. Technol.* 36(2): 35-45. <https://doi.org/10.52339/tjet.v36i2.536>
- Kiwelu, H. M. 2019. Experimental Study on the Effect of Moisture on Bolt Embedment and Connection Loaded Parallel to Grain for Timber Structures. *Tanzania J. Eng. Technol.* 38(1): 47-59. <https://doi.org/10.52339/tjet.v38i1.495>
- Magistris, F, and Salmen L, 2008 Finite Element modelling of wood cell deformation transverse to the fibre axis *Nord. Pulp Paper Res. J.* 23(2):240-246
- Structural glued-laminated timber 2010 CSA Standard 0122-06, CSA, Toronto, Ontario.

- Smith I, Kiwelu H, Weckendorf J 2015 Explanation of Tension-Side Notch Design Provisions for Glulam in CSA Standard. *Can. J. Civil Eng* cje-2015-0088R2
- Smith I, Landis E and Gong M 2003. *Fracture and fatigue in wood*, John Wiley and Sons, Chichester, United Kingdom
- Weckendorf J, Kiwelu HM, and Smith I 2015 Critical Reaction Forces of Glulam Members with tension-side notches at end supports, *Can. J. Civil Eng.* 42 (2015). <https://doi.org/10.1139/cjce-2015-0088>
- Zhang C, Huang HY, Li XY, Xue SD, Chang WS, Sun GJ 2023 Reinforcement of timber dowel-Type Connections Using Self-Tapping Screws and the Influence of Thread Configurations. *Forests* 14(2):409. <https://doi.org/10.3390/f14020409>